Adsorption 5, 25–37 (1999)

# Sorption Equilibria and Kinetics of Hydrocarbons onto Activated Carbon Samples Having Different Micropore Size Distributions

K. WANG AND D.D. DO
*Department of Chemical Engineering, The University of Queensland, Brisbane, QLD 4072, Australia*

**Abstract.** This paper deals with the prediction of adsorption equilibrium and kinetics of hydrocarbons onto activated carbon samples having different micropore size distribution (MPSD). The microporous structure of activated carbon is characterised by the distribution of slit-shaped micropores, which is assumed to be the sole source of surface heterogeneity. The interaction between adsorbate molecule and pore walls is described by the Lennard-Jones potential theory. Different adsorbates have access to different pore size range of activated carbon due to the size exclusion, a phenomenon could have a significant influence on both multicomponent equilibria and kinetics. Activated carbons with three different MPSDs are studied with ethane and propane as the two model adsorbates. The Heterogeneous Macropore Surface Diffusion model (HMSD) is employed to simulate adsorption kinetics. The simulation results show that the MPSD is an important factor affecting both the multicomponent equilibria and kinetics.

**Keywords:** micropore size distribution, activated carbon, adsorption, desorption, equilibrium, kinetics

## 1. Introduction

The structure of activated carbon is known to be very complicated. Microscopically, it is composed of two parts: the macroporous/mesoporous amorphous carbon and microporous graphite crystals. In an adsorption process, the former provides the pore space for intra-particle transport and the latter accommodates the slit-shaped micropores in which most of the adsorption capacities reside. This microporous network of the graphitic crystals dictates the overall adsorption equilibria, and together with the macropore/mesopore network they affect the overall kinetics of adsorbates into activated carbon. Because of the complex structure of activated carbon, the carbon industries have various preparation processes to produce activated carbon specific to specific applications, for example to maximise the adsorption capacity the activated carbon sample must have as large a micropore volume as possible, perhaps at the expense of the macropore volume. In applications such as liquid phase processes with large adsorbate molecules, more attention is put on the optimisation of the mesopore space as micropore volume becomes useless in those applications. In gas phase applications, the activated carbon is called optimum when it has high adsorption capacity in the micropores, and the mesopore and macropore network is such that the diffusion transport is not too restricted. The penetration of concentration front into the particle is dictated by the capacity of the solid; thus the adsorption capacity is the prime factor to be considered in the optimisation of activated carbon. It is, therefore, the objective of this paper to study the effect of micropore size distribution on the adsorption behaviour, both in equilibria and kinetics. To achieve this goal, we study three different samples of activated carbon and each of them has different micropore size distribution. The differences in the micropore size distributions of the three activated carbon samples are very small, but we will show in this paper that they will give rise to significant differences in adsorption capacity and kinetics.

## 2. Theory

The adsorption energetic heterogeneity commonly observed on activated carbon is induced by the structural heterogeneity, which can be characterised by the distribution of the slit-shaped micropores (MPSD). This

MPSD is the intrinsic property of the activated carbon and dictates the adsorption equilibria and kinetics of different adsorbate molecules on the activated carbon through the adsorbate-pore interaction. We will address our problem by first considering the single component kinetics, then multicomponent kinetics and finally to the multicomponent adsorption kinetics.

## *2.1. Single Component Equilibria*

The surface heterogeneity of activated carbon can be treated as either energetically patch-wise or structurally patch-wise (Myers, 1984). If the MPSD of the activated carbon is represented by $f(r)$ with $f(r)\,dr$ being the fraction of the micropore volumes having half-width between $r$ and $r + dr$, and the local isotherm is represented by $\theta(r)$, the overall adsorption equilibria of a species '$k$' at a pressure $P$ and temperature $T$ can be expressed as the integral of the local isotherm over the complete micropore range (Hu and Do, 1993):

$$\langle \theta_k \rangle = \int_{a_k}^{r_{\max}} \theta_k(P, r)\, f(r)\, dr \tag{1}$$

where $r_{\max}$ is the maximum micropore half-with, and $a_k$ is the minimum pore half-width below which that species can not penetrate.

Our theoretical analysis will be restricted to systems where the adsorbate-adsorbent interaction is much stronger than the adsorbate-adsorbate interaction. With this restriction, the local adsorption isotherm can take the form of the Langmuir equation:

$$\theta_k(P; r) = \frac{b_k(r) P}{1 + b_k(r) P} \tag{2}$$

where $b_k(r)$ is the local adsorption affinity characterising the strength of affinity between the adsorbate '$k$' and the adsorbent. It is a function of the local micropore half-width '$r$', and this dependence is reflected through the energy of interaction $E_k(r)$ as follows.

$$b_k(r) = b_{\infty,k} \exp\left( \frac{E_k(r)}{RT} \right) \tag{3}$$

where $b_\infty, k$ is the adsorption affinity at infinite temperature of the species '$k$' and this parameter will be further discussed later.

***2.1.1. Interaction Energy and the Pore Half-Width.*** The interaction energy between adsorbate and carbon surface, $E_k(r)$, is taken as the negative of the potential energy minimum of an adsorbate molecule interacting with all the surface atoms on the pore walls. Since we assume that the interaction between the adsorbate and the adsorbent is much stronger than the interaction energy among the adsorbed molecules, the potential energy profile between a particular adsorbate molecule and the pore is unaffected by the number of adsorbate molecules inside that pore. In other words, the energy of interaction $E_k(r)$ is independent of the fractional loading.

To obtain the potential energy profile between an adsorbate molecule and the pore, the slit-shaped micropores are assumed to consist of two sets of layers, each set of which has many lattice layers of infinite extent separated by the uniform spacing $\Delta$. With this assumption, the 10-4-3 potential energy function (Steele, 1974) is applicable and the adsorption potential energy $\varphi_k$ of species '$k$' in the pore with half width '$r$' is:

$$\begin{aligned}\varphi_k(z, r) = \frac{5}{3}\varepsilon_k^* \Bigg\{ & \frac{2}{5}\left[ \frac{\sigma_{sk}^{10}}{(r+z)^{10}} + \frac{\sigma_{sk}^{10}}{(r-z)^{10}} \right] \\ & - \left[ \frac{\sigma_{sk}^{4}}{(r+z)^{4}} + \frac{\sigma_{sk}^{4}}{(r-z)^{4}} \right] \\ & - \left[ \frac{\sigma_{sk}^{4}}{3\Delta\,[0.61\,\Delta + r + z]^3} \right. \\ & \left. + \frac{\sigma_{sk}^{4}}{3\Delta\,[0.61\,\Delta + r - z]^3} \right] \Bigg\}\end{aligned} \tag{4a}$$

where

$$\varepsilon_k^* = \frac{6}{5}\pi \rho_s \varepsilon_{sk} \sigma_{sk}^2 \Delta \tag{4b}$$

is the minimum interaction energy between the species '$k$' and a single lattice layer, $z$ is the distance between adsorbate and the central plane of the pore, $\rho_s$ is the number density of carbon molecules per unit volume. The average values of $\Delta$ and $\rho_s$ are taken as 0.335 nm and 114 nm$^{-3}$, respectively (Steele, 1974). The parameters $\varepsilon_{sk}$ and $\sigma_{sk}$ are the cross Lennard-Jones parameters for adsorbate-adsorbent interaction, which can be calculated using a geometric mean and arithmetic mean (Lorentz-Berthelot rule):

$$\begin{aligned} \varepsilon_{sk} &= \sqrt{\varepsilon_s \times \varepsilon_k} \\ \sigma_{sk} &= \frac{\sigma_s + \sigma_k}{2} \end{aligned} \tag{4c}$$

Solving Eqs. (4) for the minimum potential energy and taking the negative of which as the interaction energy, then the local interaction energy, $E_k(r)$, can be evaluated in terms of pore size over the whole MPSD range of interest.

The lower limit of the integration $a_k$ of Eq. (1) takes the half-width of pores in which the adsorbate '$k$' has the same interaction energy as its interaction with a single surface. The adsorbate would preferentially adsorb on flat surface (macro/mesopores) if the pore half-width is less than $a_k$; or in other words the adsorbate is excluded from pores having the half-width less than $a_k$. For the 10- 4-3 potential, $a_k$ depends on the size of the adsorbate molecule and can be obtained by numerically solving Eqs. (4).

Knowing the relationship between the interaction energy, $E_k(r)$, and the pore half-width $(r)$, the corresponding adsorption energy distribution (ED) of adsorbate '$k$' for a given MPSD can be calculated from the following expression (Wang et al., 1997):

$$F(E)dE = f(r)\,dr \tag{5}$$

In this work, we shall assume that the micropore size distribution takes the form of the Gamma distribution:

$$f(r) = \frac{q^{\gamma+1} r^{\gamma} e^{-qr}}{\Gamma(\gamma+1)} \tag{6a}$$

which has the following mean and variance:

$$\bar{r} = (\gamma+1)/q \tag{6b}$$

$$\sigma^2 = (\gamma+1)/q^2 \tag{6c}$$

For a given pore of half-width '$r$' exposed to an environment of species '$k$' having a pressure of $P$, the interaction energy is calculated from the potential minimum of Eqs. (4) using the information of the molecular diameter $\sigma_k$ and the minimum energy of interaction between that species and a single lattice layer, $\varepsilon_k^*$. Then the affinity is calculated according to Eq. (3) and the local adsorption isotherm can be inferred from Eq. (2). The overall adsorption equilibria is then evaluated from Eq. (1).

In this study, ethane and propane are taken as the two model adsorbates, of which the molecular properties are taken from Breck (1974) and Bird et al. (1962). These parameters, together with the calculated parameters, $\varepsilon_k^*$ and $a_k$, are listed in Table 1 for the 10-4-3 potential.

*Table 1.* The Lennard-Jones parameters for ethane and propane.

| Adsorbate | $\varepsilon_k^*$ (kJ/mol) | $\varepsilon/\kappa$ (K) | $\sigma_k$ (Å) | $a_k$ (Å) |
|---|---|---|---|---|
| Ethane | 12.80 | 230.0 | 3.91 | 3.210 |
| Propane | 14.96 | 254.0 | 4.30 | 3.382 |

#### 2.1.2. The Adsorption Affinity at Infinite Temperature.

Let us now address the adsorption affinity at infinite temperature. We shall assume that the rate of adsorption is related to the molecular collision rate toward the surface of the micropore mouth, and this collision rate is known from the kinetics theory of gases that it is inversely proportional to the square root of molecular weight and to the square root of temperature, the $b_{\infty,k}$ of the species '$k$' is given by:

$$b_{\infty,k} = \frac{\beta}{\sqrt{M_k T}} \tag{7}$$

where $\beta$ is regarded as the affinity parameter specific only to the adsorbent, whose value is affected by the lumped effects of the properties of carbon surface, such as configuration of micropores, functional groups, defects in graphite layers, pore connectivity, etc. In our previous study (Do and Do, 1997), this parameter for the Ajax activated carbon has been found to have the value of:

$$\beta = 1.3 \times 10^{-4} (\mathrm{K} \times \mathrm{g/mol})^{1/2}/\mathrm{kPa} \tag{8}$$

which is about 1/3 of the theoretical value reported by Hobson (1965).

### 2.2. The MPSDs of Sample Carbons

In the present work, we study three activated carbon samples characterised by different MPSDs. The MPSDs of these three samples take the form of the Gamma distribution, and these distributions are assumed to have the same variance but their means are different. The MPSD of the sample #2 is that of the Ajax activated carbon used in our laboratories (Wang and Do, 1997). This sample has a mean pore half-width of 4.55 Å and a variance of 0.45 Å. The samples #1 and #3 have the same variance as the sample #2, and their mean pore half-widths are 4.05 and 4.96 Å, respectively. The relevant structural parameters for these samples are tabulated in Table 2.

*Table 2.* The structural parameters of the activated carbon samples.

| Sample no. | $q$ (Å$^{-1}$) | $\gamma$ | Mean pore half-width (Å) | Variance (Å) |
|---|---|---|---|---|
| 1 | 20 | 80 | 4.05 | 0.45 |
| 2 | 22.2 | 100 | 4.55 | 0.45 |
| 3 | 24.4 | 120 | 4.96 | 0.45 |

### 2.3. *Multicomponent Equilibria*

The adsorption equilibria of a multicomponent mixture is more complicated than that of a single component system because the whole microporous network of the activated carbon may not be completely accessible to all adsorbates in the system. It is possible that there exists a certain pore range that adsorbates with larger molecular size can not penetrate (size exclusion) but which is accessible to the adsorbates with smaller molecular sizes. Let us assign the adsorbate with smallest molecular size as the species 1 and the largest adsorbate as $N$ in the $N$-component system. The adsorption equilibria of the species '$k$' is given by the following equation:

$$\begin{aligned}\langle\theta_k\rangle = &\int_{a_k}^{a_{k+1}} \theta_k^{(k)}(P_1, P_2, \ldots, P_k; r)\, f(r)\, dr \\ &+ \int_{a_{k+1}}^{a_{k+2}} \theta_k^{(k+1)}(P_1, P_2, \ldots, P_k, P_{k+1}; r)\, f(r)\, dr \\ &+ \cdots \int_{a_N}^{r_{\max}} \theta_k^{(N)}(P_1, P_2, \ldots, P_k, \ldots, P_N; r) \\ &\times f(r)\, dr, \qquad (k = 1, 2, \ldots, N) \quad (9)\end{aligned}$$

where $\theta_k(\underline{P}, r)$ is the local adsorption isotherm and it can be represented by the extended Langmuir equation:

$$\theta_k^{(M)}(P_1, P_2, \ldots, P_M; r) = \frac{b_k(r) P_k}{1 + \sum_{j=1}^{M} b_j(r) P_j}, \qquad M \le N; \quad M = k, k+1, \ldots, N \qquad (10)$$

The first term in the RHS of Eq. (9) is the contribution to the adsorption of species '$k$' by the range of pores that are accessible to species 1 to species $k$, the second term is the contribution by the range of pores that are accessible to species 1 to species $k + 1$, and the last term is the contribution by the range of pores that are accessible to all species. Thus the size exclusion effect is accounted for in the overall isotherm equation.

For multicomponent systems containing $N$ different adsorbates adsorbing onto a heterogeneous surface, the competition of different adsorbates for adsorption space within the micropore is a fundamental problem. Equation (9) states that the competition between different adsorbates is local to each pore, that is if a pore of size $r_A$ accommodates only adsorbates 1 and 2, then the competition is restricted to those two adsorbates only. Other adsorbates inaccessible to that pore *do not* participate in the competition, and hence are not accounted for in the local extended Langmuir equation for that pore. This concept of adsorbates-pore interaction is more fundamental than the traditional approach of cumulative energy matching between different species (Valenzuela et al., 1988):

$$\frac{E(i) - E_{\min}(i)}{E_{\max}(i) - E_{\min}(i)} = \frac{E(j) - E_{\min}(j)}{E_{\max}(j) - E_{\min}(j)}, \qquad i, j = 1, 2, 3, \ldots, N \quad (11)$$

whereby the matching does not bring out the feature of competition of adsorbates residing in a pore. Furthermore, matching the energies of two species may occur over two pores of different sizes, which is physically impossible. We shall discuss this point in the discussion section.

### 2.4. *MPSD and Adsorption Kinetics*

In dealing with the adsorption kinetics, we will assume that the activated carbon samples are of a size such that the rates of adsorption into the micropores and desorption from those pores are much faster than the diffusion rates of the free species and the adsorbed species along the particle coordinate. This amounts to saying that at any point within the particle the fluid phase is in equilibrium with the adsorbed phase, i.e., there exists a relationship between the partial pressure and the adsorbed phase concentration according to the local isotherm equation (Eq. (10)).

***2.4.1. Surface Diffusion Flux.*** With the driving force for surface diffusion being taken as the gradient of chemical potential, which is equal to the chemical potential of that species in bulk phase, the local surface diffusion flux of species ‘$k$’ can be expressed as:

$$J_\mu(r,k) = -D_\mu^0(r,k)\frac{C_\mu(r,k)}{C(k)}\frac{\partial C(k)}{\partial Z} \tag{12}$$

where $D_\mu^0(r,k)$ is the surface diffusivity of species ‘$k$’ at zero coverage, and is defined in terms of local activation energy for surface diffusion as:

$$D_\mu^0(r,k) = D_{\mu\infty}^0(k)\exp\left(-\frac{aE(r,k)}{R_g T}\right) \tag{13}$$

where ‘$a$’ is the ratio of activation energy for surface diffusion to the adsorption energy $E(r,k)$ and $D_{\mu\infty}^0$ is the surface diffusivity at zero coverage and infinite temperature level, which reflects the mobility of adsorbate molecule on certain adsorbent at the extreme conditions.

***2.4.2. The Mass Balance Equation.*** With above definitions and assumptions, the Heterogeneous, Macropore, Surface Diffusion model (HMSD) previously proposed by Do and Hu (1993) is applicable here to describe the adsorption kinetics. The overall mass balance equation for a particle can be expressed in terms of the gas phase concentration ‘$C$’ and the MPSD as:

$$\begin{aligned}\{\varepsilon + (1-\varepsilon)H[k, C(k)]\}\frac{\partial C(k)}{\partial t} \\ = \frac{1}{Z^s}\frac{\partial}{\partial Z}\left\{Z^s D_c[k, C(k)]\frac{\partial C(k)}{\partial Z}\right\}\end{aligned} \tag{14a}$$

with

$$H[k, C(k)] = \int_{a_k}^{r_{\max}} \frac{C_{\mu s}(k)b(r,k)}{\left[1+\sum_{j=1}^N b(r,j)C(j)\right]^2} f(r)\,dr \tag{14b}$$

$$\begin{aligned}D_c[k, C(k)] = \varepsilon D_p(k) + (1-\varepsilon)\int_{a_k}^{r_{\max}} D_{\mu\infty}^0(k) \\ \times \frac{C_{\mu s}(k)b(r,k)}{\left[1+\sum_{j=1}^N b(r,j)C(j)\right]} f(r)\,dr\end{aligned} \tag{14c}$$

where $\varepsilon$ is the macroporosity of the particle. In the above equation, the bulk diffusion flux is represented by the Fickian form:

$$J_p(k) = -D_p(k)\frac{\partial C(k)}{\partial Z} \tag{14d}$$

where $D_p$ is the pore diffusivity (Ruthven, 1984).

The boundary and initial conditions for the model equations are:

$$Z = 0; \quad \frac{\partial C(k)}{\partial Z} = 0 \tag{15a}$$

$$\begin{aligned}Z = R; \quad \varepsilon J_p(k) + (1-\varepsilon)\int_{a_k}^{r_{\max}} J_\mu(r,k) f(r)\,dr \\ = k_m(k)[C(k) - C_b(k)]\end{aligned} \tag{15b}$$

$$t = 0^+; \quad C = C_0;$$

$$C_{\mu 0}(k) = C_{\mu s}(k)\int_{a_k}^{r_{\max}} \frac{b(r,k)C_0(k)}{1+\sum_{j=1}^N b(r,j)C_0(k)} f(r)\,dr \tag{15c}$$

The above model assumes a parallel path mechanism (PPM) in terms of pore sizes (Kapoor and Yang, 1989), in which the overall surface flux of species ‘$k$’, $J_\mu^k$, is the summation of the local surface fluxes, $J_\mu^k(r)$, contributed by all micropores accessible to that species, i.e.,

$$\begin{aligned}\langle J_\mu^k\rangle = &\int_{a_k}^{a_{k+1}} J_\mu^k(C_1, C_2, \ldots, C_k; r) f(r)\,dr \\ &+ \int_{a_{k+1}}^{a_{k+2}} J_\mu^k(C_1, C_2, \ldots, C_k, C_{k+1}; r) f(r)\,dr \\ &+ \cdots \int_{a_N}^{r_{\max}} J_\mu^k(C_1, C_2, \ldots, C_k, \ldots, C_N; r) \\ &\times f(r)\,dr\end{aligned} \tag{16}$$

Equation (16) is similar in form to Eq. (9) in that the local adsorption equilibria, $\theta_k(r)$, is replaced by the local surface flux, $J_\mu^k(r)$. So the effect of size exclusion and the ‘adsorbate-pore interaction’ mechanism described before are also incorporated in the HMSD model.

## 3. Simulation Parameters and Methodology

The multicomponent equilibria and kinetics models described in the previous section require only parameters associated with the single component systems. We do this by fitting the models with single component systems of one particular activated carbon sample. Once this is done, the simulation of the models for other activated carbon samples can be carried out. For the simulation results to bear any reliability, it is important that parameters are defined such that they can be either functions of the adsorbate properties or functions of the characteristics of the solid surface. The only parameter we allow to vary from one sample to the others is the micropore size distribution.

In the present work, three sets of basic equilibrium and kinetics parameters independent of the MPSD of carbon samples are:

1. the minimum interaction energies between a species and a single graphitic layer, $\varepsilon_k^*$;
2. the affinity parameter, $\beta$, and
3. the surface diffusivity at zero loading and infinite temperature, $D_{\mu\infty}^0$.

Let us now discuss the significance of these parameters. The first parameter depends only on the properties of the adsorbate molecule and the surface atom (Eq. (4b)) and therefore for a given adsorbate it can be used for all samples of activated carbon. The second parameter $\beta$ (Eq. (7)) is the adsorption affinity at infinite temperature. This parameter is taken as independent of adsorbate, and is a function of the nature of the micropore mouth, and this is again assumed the same for all samples. Testing this with two different commercial activated carbon samples, we have found that this parameter is almost independent of the adsorbent (Do and Do, 1997). The third parameter is the surface diffusivity at infinite temperature, and we shall assume that it is independent of adsorbates. These arguments are supported by our previous studies on equilibria and kinetics experimental data of various adsorbates (including hydrocarbon, aromatics, $CO_2$, and $SO_2$) on Ajax activated carbon (Do and Wang, 1997). These parameters are listed in the following table, obtained from the extensive fitting of experimental data on Ajax activated carbon.

It is noted that the values of $\varepsilon_k^*$ in Table 3 are very comparable to the theoretical values in Table 1 (within the error of 10%). This good agreement is also found in the adsorption of other hydrocarbon gases/vapours on activated carbon (Wang and Do, 1997), for which the assumption that the adsorbate-adsorbent interaction is much stronger than the adsorbate-adsorbate interaction is valid.

*Table 3.* The basic equilibria and kinetics parameters for simulation.

| | $\varepsilon_k^*$ (kJ/mol) | $\beta$ ((g × K)$^{1/2}$/kPa) | $D_{\mu\infty}^0$ (m$^2$/s) | $C_{\mu s}$ (mmol/g) |
|---|---|---|---|---|
| Ethane | 13.8 | $1.3 \times 10^{-4}$ | $3.5 \times 10^{-7}$ | 8 |
| Propane | 16.0 | $1.3 \times 10^{-4}$ | $3.5 \times 10^{-7}$ | 6 |

With all the basic parameters defined as shown in Table 3, the adsorption equilibria can be simulated for activated carbon samples having different micropore size distribution (Eq. (9)) to study the effect of the MPSD on the adsorption equilibria. The simulation for kinetics of ethane and propane on the three samples of activated carbon is done by solving Eqs. (14) and (15). The kinetic model equations are in the form of coupled partial differential equations, and they are solved using the following procedure:

1. The model equations are non-dimensionalised in time and space domains and then transformed into a larger set of ODEs by applying the orthogonal collocation technique (Do and Hu, 1993)
2. The resulted ODEs are then solved numerically by the integration package in MATLAB.

The detailed procedures and solution methodology can be found elsewhere (Do and Hu, 1993). All the simulations are performed on a Pentium desktop computer with a clock speed of 133 MHz. The simulation takes about several seconds for single component equilibrium to several minutes for multicomponent kinetics in each run.

## 4. Results and Discussion

### 4.1. *The MPSDs of Three Activated Carbon Samples*

The aim of this study is to investigate the role of MPSD in the overall adsorption equilibrium and kinetics on the heterogeneous surface of activated carbon and this is achieved by comparing the simulation results of adsorption equilibria and kinetics of the model adsorbates on sample carbons with different MPSDs. Figure 1 shows graphically the MPSD of each activated carbon sample with their structural parameters given in Table 2. It can be seen that the distribution profiles of these activated carbon samples (hereafter referred to as AC1, AC2 and AC3) have the same variance but different means, with AC1 being the sample with the smallest average pore size and AC3 having the largest average pore size. Also shown in Fig. 1 are the minimum pore

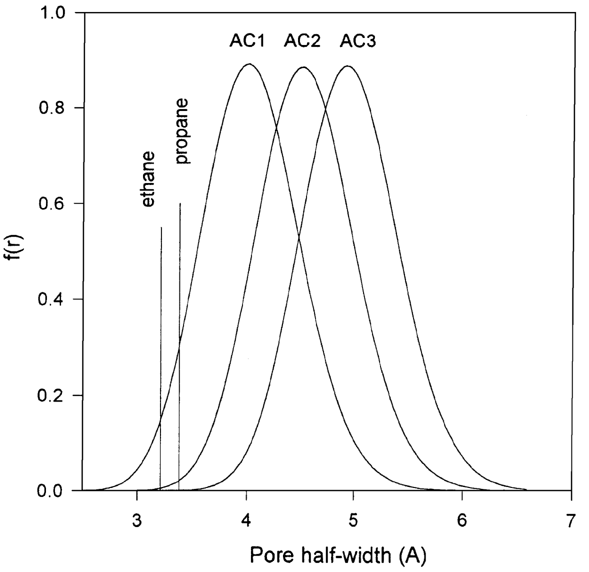

*Figure 1.* The micropore size distribution (MPSD) of each sample carbon and pore accessibility cut off of each species.

half widths accessible to ethane and propane ($a_k$). We see that AC2 and AC3 have all their pores available to ethane and propane. The AC1 sample, on the other hand, has a portion of its micropore volume available only to ethane. This fact has a consequence in the multicomponent adsorption equilibria and kinetics as we shall see.

### 4.2. *The MPSD and Adsorption Equilibria*

***4.2.1. Single Component Systems.*** The single component adsorption equilibria of ethane and propane on each activated carbon sample are first simulated and shown in Figs. 2(a) and 2(b), respectively. The simulation temperature is 303 K. Experimental data on AC2 sample are presented in Fig. 2 as symbols. It is seen that, as the mean pore size is getting smaller (that is from AC3 to AC1 sample), the adsorbed concentration for each species increases drastically. Note that the mean pore half-width of AC1 is 4.05 while that of AC3 is 4.96 Å. The reason for this increase is that the interaction energy is enhanced due to the closer proximity of the pore walls, resulting in an increase in the adsorption affinity and thence adsorption density. The energy distributions of these activated carbon samples are calculated from Eq. (5) and the results are shown in Fig. 3. We see that the AC1 sample has higher density in the high energy range while the sample AC3 has higher density in the lower energy range; thus the AC1 gives better adsorption capacity than AC3 as we have already seen in Fig. 2. One thing we also note from Fig. 3 is that only a small change in the MPSD has resulted in a very large change in the energy distribution. This means that tailoring of activated carbon to suit a specific application is a delicate operation.

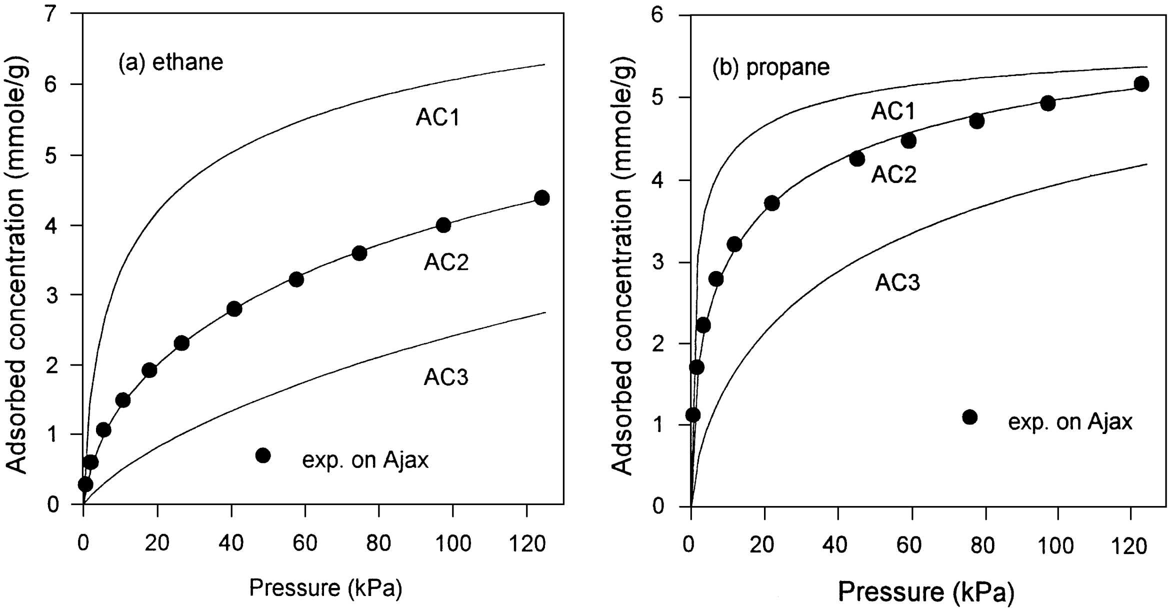

*Figure 2.* The single component adsorption equilibria on each sample carbon at 303 K. (a) ethane; (b) propane.

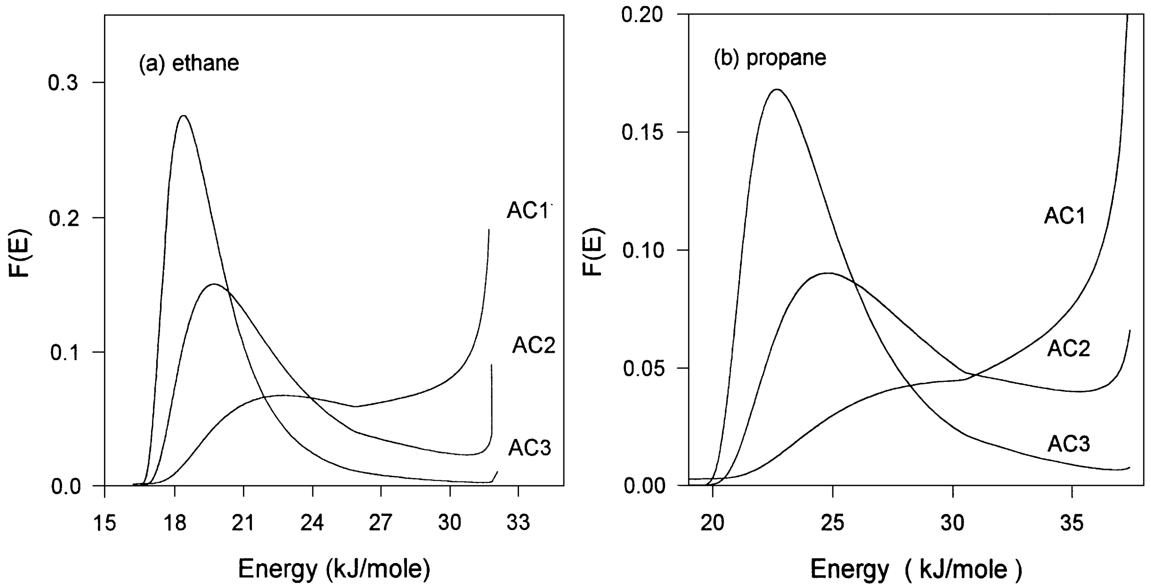

*Figure 3.* Adsorption energy distribution (ED) on each sample carbon. (a) ethane; (b) propane.

***4.2.2. Multicomponent Systems.*** For single component system adsorbing onto a heterogeneous surface, the adsorption equilibria can be simulated by using either the MPSD or the induced energy distribution (ED) as the measure of the surface heterogeneity. The results are identical because of the induced energy is calculated directly from the MPSD (Eq. (5)). For multicomponent system, however, the situation becomes more complicated. When using the micropore size distribution (MPSD) in the calculation of multicomponent adsorption kinetics, the procedure for the calculation of equilibria is straightforward as we have shown in the theory section. Using the ED approach where we use the matching of the cumulative energy of different adsorbates as the relationship between their energies of interaction, the problem is that the matching does not bring out the feature of competition of adsorbates residing in a pore. Furthermore matching the energies of two species may occur when each of the adsorbates resides in pores of different size, which is physically impossible.

In the MPSD approach, only those adsorbates present in the pore are available for competition for the adsorption space of that pore. This is what we call the excluded adsorbates-pore competition. Because of the exclusion of large adsorbate molecules from some pores, the calculation of the multicomponent adsorption isotherm must be carried out in regions as we have shown mathematically in Eq. (9). We shall illustrate this point in Fig. 4 where we plot the interaction energy between ethane and the pore of half-width $r$, calculated from the 10-4-3 potential. The interaction energy between propane and the pore is also shown on the same figure. This figure is used to determine the interaction energies of adsorbates within a specific

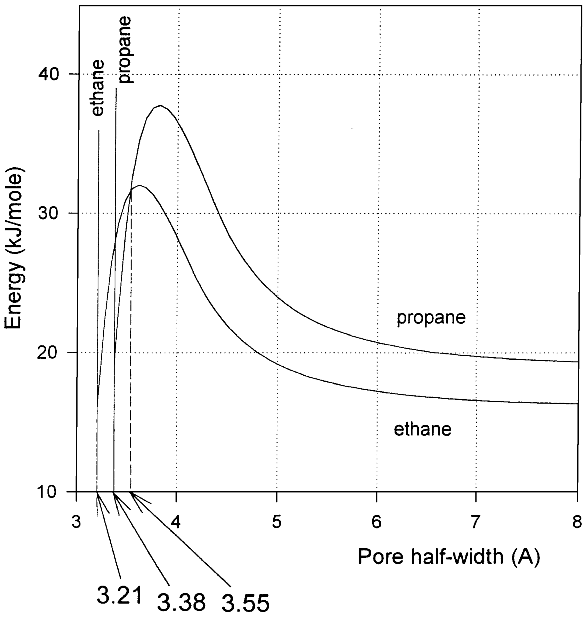

*Figure 4.* The ethane-propane interaction energy matching as the function of micropore size.

*Table 4.* Interaction energies of ethane and propane evaluated at the mean pore half-width for the three activated carbon samples (AC1, AC2, and AC3).

| Species | (AC1) $r = 4.05$ | (AC2) $r = 4.55$ | (AC3) $r = 4.96$ |
|---|---|---|---|
| Ethane | 27.43 | 21.51 | 19.32 |
| Propane | 35.85 | 27.87 | 24.18 |

pore. For example, in a pore of half-width 4.05 Å of the sample AC1, the interaction energies of ethane and propane are 27.4 and 35.9 kJ/mol, respectively. For the other two samples, the interaction energies (kJ/mol) at the mean pore half-width are tabulated in Table 4.

From Fig. 4 we see that for pores having half-width between 3.21 and 3.38 Å only ethane is allowed to enter the pore while propane is excluded. Both ethane and propane can adsorb in pores having half-width larger than 3.38 Å. What is also interesting is that in pores having half-width between 3.38 and 3.55 Å, ethane actually has higher affinity than propane, and only in pores with half-width greater than 3.35 Å that propane will have higher adsorption affinity than ethane. We summarise this observation in Table 5.

*Table 5.* Accessibility of ethane and propane and their relative adsorption affinity.

| Pore range | Ethane | Propane | Relative affinity |
|---|---|---|---|
| $3.21 < r < 3.38$ Å | Allowed | Excluded | Ethane by itself |
| $3.38 < r < 3.55$ Å | Allowed | Allowed | Ethane > propane |
| 3.55 Å $< r$ | Allowed | Allowed | Propane > ethane |

It can be seen that, in pores with different sizes, the interaction energy is a complicated problem as we have summarised in the above table. The traditional approach of cumulative energy matching given in Eq. (11) is an oversimplified solution and can be physically incorrect. For example, the highest energies in the three carbon samples are 32 kJ/mol for ethane and 37 kJ/mol for propane (Fig. 2). In matching these energies in the cumulative energy approach leads to serious error because the pores corresponding to these energies having widths of 7.3 and 7.7 Å, respectively. It is impossible to have competition of ethane and propane when each one of these are in pores of different size!

Figures 5(a), (b), and (c) show the simulated binary adsorption equilibria of ethane (30%) and propane (70%) as a function of total pressure for each activated carbon sample. The temperature is 303 K. The solid lines represent the simulation results from the MPSD approach and the dashed lines represent the results from ED approach. It is seen that, on AC2 and AC3, the MPSD approach predicts higher adsorbed concentration for stronger adsorbing species and lower concentration for weaker adsorbing species than ED does. This is the due to the problem associated with the matching of cumulative energy approach as we have mentioned earlier.

To further understand the effect of different MPSD on the binary equilibria, we calculate the selectivity of ethane as follows.

$$S_{\text{ethane/propane}} = \frac{(X_{\text{ads}}/Y_{\text{bulk}})_{\text{ethane}}}{(X_{\text{ads}}/Y_{\text{bulk}})_{\text{propane}}} \tag{17}$$

Figure 6 shows this selectivity for ethane versus the total pressure for the three activated carbon samples.

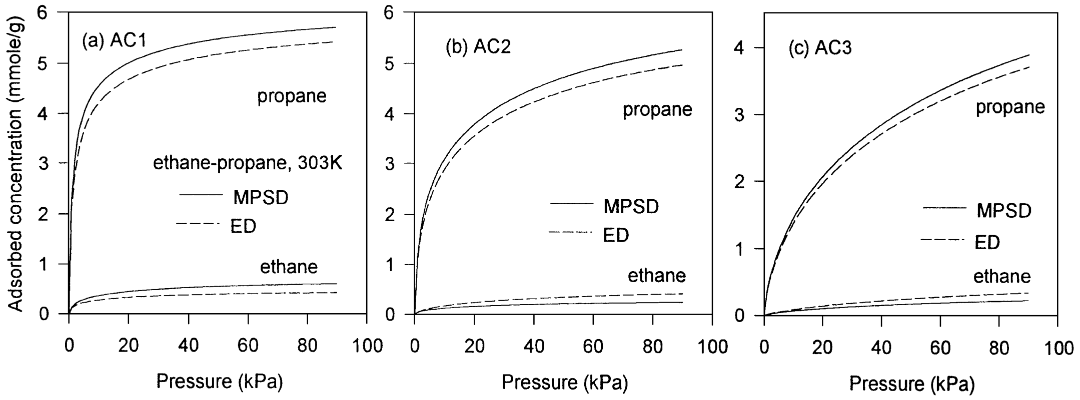

*Figure 5.* The multicomponent adsorption equilibria of ethane (30%)-propane (70%) mixture on each sample carbon at 303 K. (a) AC1; (b) AC2; (c) AC3.

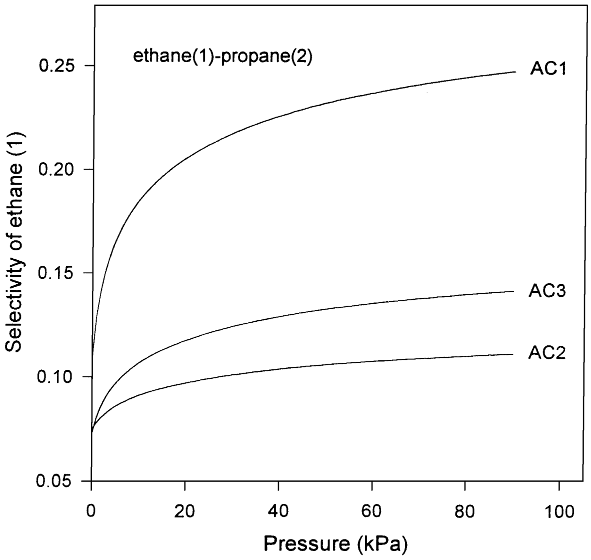

*Figure 6.* The equilibrium selectivity of ethane in ethane (30%)-propane (70%) mixture as a function of bulk pressure.

We see that the selectivity for ethane decreases when we move from the large pore size sample (AC3) to the smaller pore size sample (AC2). This is explained as follows. The interaction energies of ethane evaluated at the mean pore half-width of AC3 to AC2 are 19.3–21.5 kJ/mol, respectively (Table 4). Therefore the increase in the adsorption affinity of ethane when we move from AC3 to AC2 is:

$$\exp\left(\frac{21500}{RT}\right)\Big/\exp\left(\frac{19300}{RT}\right) = 2.4$$

For propane, the corresponding interaction energies are 24.2 and 27.9 kJ/mol for AC3 and AC2, respectively; thus an increase in the adsorption affinity is 4.3, which is greater than that for ethane. What this means is that the activated carbon sample is more favourable towards propane when we move from AC3 to AC2; hence a drop in the selectivity for ethane as we have seen in Fig. 6. This trend, however, is not observed when we move from AC2 to AC1. Using the interaction energies in Table 4, we calculate the increase in the adsorption affinity. This increase for ethane is 3.2 while that for propane is 24. One would then expect that the selectivity for ethane is further reduced because AC1 has more affinity towards propane than to ethane, but what we see in Fig. 6 is the opposite; we see an increase in the ethane selectivity instead. This is due to the exclusion phenomenon as in AC1 there is a fraction of its micropore volume, having half-width between 3.21 and 3.38 Å, which is inaccessible to propane. Furthermore, there is another fraction of micropore volume, having half-width between 3.38 and 3.35 Å, where ethane has higher affinity than propane. Therefore ethane has more volume for adsorption in AC1 than propane does and it has higher affinity in some pores, resulting in an increase in the ethane selectivity for AC1 compared to AC2.

### 4.3. The MPSD and Adsorption Kinetics

**4.3.1. Single Component Kinetics.** The simulation of sorption kinetics are carried out with activated carbon samples having slab geometry and a full length of 4.4 mm. The porosity of the transport pores is 0.31. The conditions of the system are 303 K and 1 atm total pressure. The bulk diffusivity for ethane and propane are $1.68 \times 10^{-6}$ and $1.30 \times 10^{-6}$ ($m^2/s$), respectively. The ratio of activation energy for surface diffusion to adsorption energy is assumed to be 0.5.

Figure 7(a) shows the single component adsorption as well as desorption kinetics of 5% ethane on each AC. The desorption curve is for the case where the particle pre-equilibrated with 5% ethane is desorbed in the environment of inert gas. It is seen that, the desorption kinetics are much more sensitive to the change of the MPSD than the adsorption kinetics. This observation is in agreement with other studies and it suggests that the desorption is better than the adsorption for the study of surface heterogeneity of activated carbon (Cerofolini and Re, 1995). This phenomenon attributes to the existence of smaller pores with higher adsorption energies in which the desorption rates are very slow. The reason why the adsorption mode is not sensitive to the adsorbent is explained as follows. The AC1 sample has higher adsorption capacity than AC2 (3 times larger in capacity) and one would expect AC1 has a substantially slower adsorption time than that for AC2 because it takes longer time to ‘fill’ high capacity adsorbent. In fact the half time for the AC1 sample is only 1.5 slower than that for the AC2 sample. This is due to the fact that the surface diffusivity increases with loading (see Eq. (13)). AC1 has higher loading and hence the surface diffusivity is higher, making the time to adsorb larger amount in shorter time than what it should be. The simulation results of the desorption kinetics of 10% propane on each AC shown in Fig. 7(b) again show that the desorption is sensitive to the variation in the MPSD.

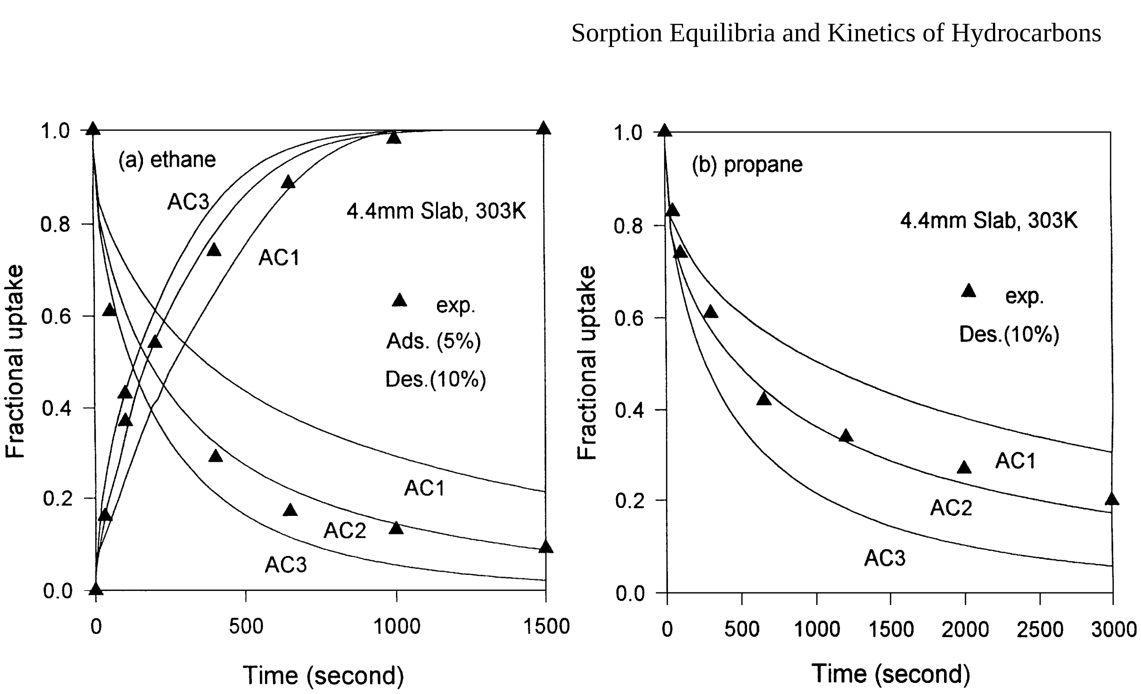

*Figure 7.* The single component sorption kinetics at 303 K on each sample carbon of 4.4 mm slab pellet. (a) ethane; (b) propane.

Experimental data of AC2 sample are shown in Figs. 7 as symbols.

***4.3.2. Multicomponent Kinetics.*** The adsorption kinetics of binary mixture of ethane(5%)-propane(5%) on 2 mm slab pellets at 283 K are then studied for each AC, and the results of the simulation and the experimental data on AC2 are shown in Figs. 8(a), (b) and (c) for the three samples of activated carbon. It is seen that, the HMSD model correctly describes the overshoot phenomena of ethane (the faster moving/less-strongly adsorbed species) by propane, the slower moving/strongly adsorbed species. Contrary to what we observed in the single component kinetics, the multicomponent adsorption kinetics is very sensitive to the changes in the MPSD.

Let us first examine the uptake time at which the maximum overshoot of ethane happens ($t_{\max}$) and the uptake time at which the final equilibrium is reached ($t_f$). As we move from AC3 to AC1, $t_{\max}$ increases from

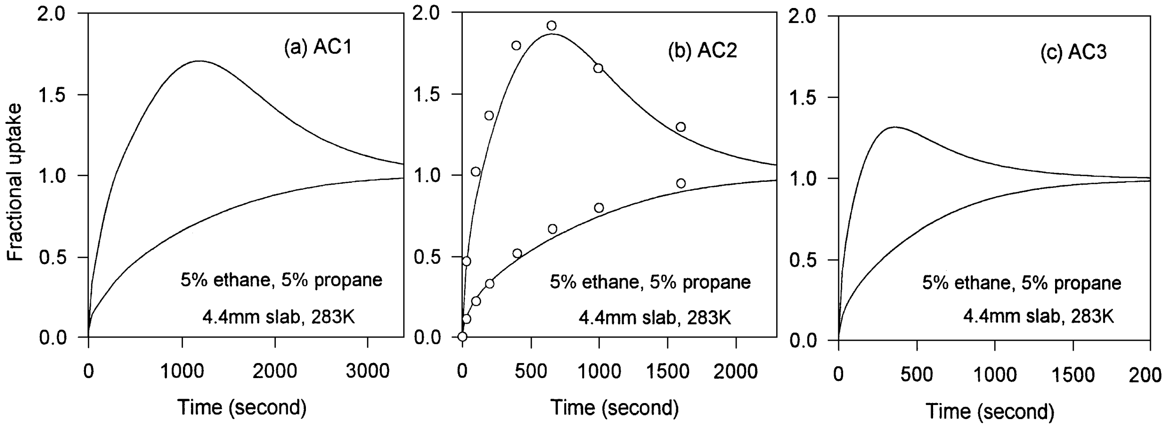

*Figure 8.* Non-dimensional adsorption kinetics of ethane (5%)-propane (5%) mixture at 283 K on each sample carbon of 4.4 mm slab. (a) AC1; (b) AC2; (c) AC3.

about 350 to about 1200 s, and $t_f$ increases from about 1500 to more than 3000 s. This suggests that, as the mean pore size decreases (or the interaction energies increase), the rate of uptake is greatly reduced. The effect of MPSD is further manifested in the overshoot degree of light species on each AC. When the MPSD shifts from AC3's to AC2's, the overshoot degree of ethane increases from 1.3 to 1.9. This behaviour is expected and typical as in AC3 and AC2 all their micropore volumes are available. Since propane has higher capacity and lower surface diffusivity, we expect an overshoot of ethane. When we move from AC3 to AC2 the rate of increase in the average energy for propane is higher than that for ethane; thus this makes the overshoots higher and the time when this occurs is also longer. As the MPSD further shifts from AC2's to AC1's, the overshoot degree of ethane drops from 1.9 to 1.7. If we apply the argument as we just did when we moved from AC3 to AC2, we would expect a further increase in the overshoot degree from 1.9 but instead we see a decrease from 1.9 to 1.7. The reason for why this happens is explained exactly the same way we explained for the multicomponent equilibria. In AC1, there is a fraction of the micropore volume in which ethane is the only species as propane is excluded from those pores, and furthermore, in pores having half-width from 3.38 to 3.55 ethane has higher affinity than propane. Therefore the degree of overshoot is lower when we shift from AC2 to AC1.

## 5. Conclusion

The role of the micropore size distribution on adsorption equilibria and kinetics are illustrated with three activated carbon samples having different MPSDs. The MPSD is regarded as the source of surface heterogeneity which dictates the adsorbate-adsorbent interaction through the Lennard-Jones 10-4-3 potential. Ethane and propane are chosen as the two model adsorbates.

The adsorbate-adsorbate interaction energy matching between different species in multicomponent system is investigated and an approach based on the adsorbate-pore interaction mechanism is proposed and employed in the simulation of the adsorption properties. Meanwhile, the traditional approach of linear energy matching is also used in simulation as a way of comparison. For the systems studied, differences are found between the simulation results of multicomponent equilibria as well as kinetics obtained from these two approaches. This is due to the serious limitation of the cumulative matching method.

The simulations show that the effect of size exclusion on overall adsorption equilibria and kinetics are very important when the mean pore size of activated carbon is small or the difference between molecular sizes is large.

## Acknowledgment

The support from the Australia Research Council (ARC) is gratefully acknowledged.

## Nomenclature

| | | |
|---|---|---|
| $a$ | Ratio of diffusion energy to adsorption energy (0.5) | — |
| $a_k$ | The minimum accessible pore half width of adsorbate '$k$' | — |
| $Bi$ | Biot number | — |
| $b_0$ | Adsorption affinity at zero energy level | $\text{kPa}^{-1}$ |
| $b_{k(r)}$ | Affinity of species $k$ at micropore with half-width '$r$' | $\text{kPa}^{-1}$ |
| $b_\infty$ | Adsorption affinity at infinite temperature | $\text{kPa}^{-1}$ |
| $C$ | Bulk phase concentration | $\text{mol/m}^3$ |
| $C_0$ | Initial gas phase concentration | $\text{mol/m}^3$ |
| $C_b$ | Bulk phase concentration of gas phase | $\text{mol/m}^3$ |
| $C_\mu$ | Adsorbed phase concentration | $\text{mol/m}^3$ |
| $C_{\mu s}$ | Maximum adsorbed phase concentration | $\text{mol/m}^3$ |
| $D_p$ | Pore diffusivity | $\text{m}^2\text{/s}$ |
| $D_\mu$ | Surface diffusivity | $\text{m}^2\text{/s}$ |
| $D^0_{\mu\infty}$ | Surface diffusivity at zero loading and zero energy level | $\text{m}^2\text{/s}$ |
| $E_{\text{mean}}$ | Average adsorption energy | J/mol |
| $E(r)$ | Adsorption energy inside the pores with half-width '$r$' | J/mol |
| HMSD | Heterogeneous Macropore, Surface diffusion model | — |

| | | |
|---|---|---|
| $J_P$ | Pore flux | mol/m$^2$/s |
| $J_\mu$ | Surface flux | mol/m$^2$/s |
| $k_m$ | Film mass transfer coefficient | m$^{-1}$ |
| $M$ | Molecular weight | g/mol |
| $q$ | Gamma distribution parameter | Å$^{-1}$ |
| $R_g$ | Gas constant | — |
| $r$ | Pore half-width | Å |
| $r_{\max}$ | Maximum pore half-width | Å |
| $s$ | Geometric factor of the particle, 0, 1, 2 for slab, cylinder and sphere, respectively | — |
| $T$ | Temperature | K |
| $t$ | Time | s |
| $z$ | Distance between adsorbate and pore wall | Å |
| $\beta$ | The affinity parameter | (K × g)$^{1/2}$/ $\mu$Pa |
| $\sigma_{sf}$ | Collision diameter between solid (carbon) molecule and fluid molecule | Å |
| $\varepsilon$ | Particle porosity | — |
| $\varphi_k(z, r)$ | Pore potentials at distance '$z$' in pore with radius '$r$' | J/mol |
| $\varepsilon_k^*$ | Interaction potential minimum for single graphite lattice | J/mol |
| $\gamma$ | Distribution parameter | — |

## References

Bird, R.B., W.E. Stewart, and E.N. Lightfoot, *Transport Phenomena*, John Wiley & Sons, New York, 1962.

Breck, D.W., *Zeolite Molecular Sieves: Structure, Chemistry and Use*, John Wiley & Sons, New York, 1974.

Cerofolini, G.F. and N. Re, "Extracting the Energy Distribution Function of Heterogeneous Surfaces from their Desorption Kinetics," *J. Colloid & Interface Sci.*, **174**, 428 (1995).

Do, D.D. and H.D. Do, "A New Adsorption Isotherm for Heterogeneous Adsorbent Based on the Isosteric Heat as a Function of Loading," *Chem. Eng. Sci.*, **52**, 297 (1997).

Do, D.D. and X. Hu, "An Energy Distribution Model for Adsorption Kinetics in Larger Heterogeneous Microporous Particle," *Chem. Eng. Sci.*, **48**, 2119 (1993).

Do, D.D. and K. Wang, "A New Model for the Description of Adsorption Kinetics in Heterogeneous Activated Carbon," *Carbon*, **36**, 1539 (1998).

Hobson, J.P., "A New Method for Finding Heterogeneous Energy Distributions from Physical Adsorption Isotherm," *J. Chem. Phys.*, **43**, 1934 (1965).

Kapoor, A. and R.T. Yang, "Surface Diffusion on Energetically Heterogeneous Surface," *AIChE J.*, **35**, 1735 (1989).

Myers, A.L., "Adsorption of Pure Gases and their Mixtures on Heterogeneous Surfaces," in *Fundamentals of Adsorption*, A.L. Myers and G. Belfort (Eds.), Engineering Foundation, New York, 1984.

Ruthven, D.M., *Principles of Adsorption and Adsorption Processes*, Wiley, New York, 1984.

Steele, W.A., *The Interaction of Gases with Solid Surface*, Pergamon, Oxford, 1974.

Valenzuela, D.P., A.L. Myers, O. Talu, and I. Zwiebel, "Adsorption of Gas Mixtures: Effect of Energetic Heterogeneity," *AIChE J.*, **34**, 397 (1988).

Wang, K., A. Ahamdpour, and D.D. Do, "Kinetics and Equilibrium Characterisation of Two Physically Nut Shell Derived Activated Carbon," *Adsorption*, **3**, 267 (1997).

Wang, K. and D.D. Do, "Characterising Micropore Size Distribution of Activated Carbon using Equilibrium Data of Many Adsorbates at Various Temperatures," *Langmuir*, **13**, 5226 (1997).